

A Modified Dynamic Model for Planar Microwave Circuits

Tullio Rozzi, *Fellow, IEEE*, Antonio Morini, Andrea Pallotta, and Franco Moglie, *Member, IEEE*

Abstract—The present work is aimed at enhancing the effectiveness of the moments method in solving planar microwave circuits problems. It stems from the same analytical model as [1], [2]. Its novelty consists in introducing a technique, of fundamental mode sampling, that substantially reduces the complexity of the analysis and the computation time involved in the characterization of all practical discontinuities. Moreover, the numerical results are in very good agreement with experimental data.

I. INTRODUCTION

THE CHARACTERIZATION of discontinuities in planar circuits for microwave frequencies requires the use of rigorous approaches that take into account all physical effects.

In [1], [2] a powerful and effective method is presented for the study of discontinuities such as the microstrip-to-slotline transition and related structures, such as the slot antenna, the microstrip open-end and the shorted slotline.

Only transverse currents are neglected, that is allowable for typical impedance levels in the microwave range; near field effects, including surface waves and radiation are included in the moments method solution. The only drawback of the method is constituted by the great numerical complexity involved in the model, that sets a practical limit to accuracy, particularly at the higher frequencies. It is therefore important to consider analytical ways of reducing the size of the above task.

II. THE BASIC MOMENTS METHOD

The method is summarized by considering the typical microstrip-to-slotline transition, whose top and cross sectional views are depicted in Figs. 1 and 2, respectively.

Neglecting, as stated, transverse electric and magnetic currents (J_z, E_z), the system of integral equations to be solved is the following:

$$\begin{aligned} & \iint J_x(x, -d, z) \omega(z') Z_{xx}^{11}(x, z; x', z') dx' dz' \\ & + \iint_{\text{slotline}}^{\text{microstrip}} E_x(x, 0, z) \delta(x') A_{xx}^{12}(x, z; x', z') dx' dz' \\ & = E_x(x, -d, z) \end{aligned} \quad (1)$$

Manuscript received April 1, 1991; revised July 31, 1991.

The authors are with Dipartimento di Elettronica ed Automatica, Università degli studi di Ancona, via Brecce Bianche, 60131 Ancona, Italy.

IEEE Log Number 9103394.

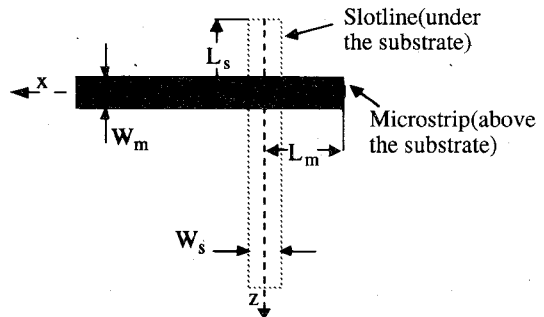


Fig. 1. Top view of microstrip-to-slotline transition.

at the microstrip interface, and

$$\begin{aligned} & \iint J_x(x, -d, z) \omega(z') A_{xx}^{21}(x, z; x', z') dx' dz' \\ & + \iint_{\text{slotline}}^{\text{microstrip}} E_x(x, 0, z) \delta(x') Y_{xx}^{22}(x, z; x', z') dx' dz' \\ & = J_x(x, 0, z) \end{aligned} \quad (2)$$

at the slotline interface.

The exact Green functions of the dielectric "slab," Z_{xx}^{11} , A_{xx}^{12} , A_{xx}^{21} , Y_{xx}^{22} , correspond respectively to the expressions (2(a)–(d)) in [2].

A fundamental step in the application of the moments method is constituted by the choice of the set of separable functions in terms of which the above system of integral equation is discretized, namely,

$$J_x(x, -d, z) = E(x) \omega(z) \quad (3)$$

$$E_x(x, 0, z) = M(z) \delta(x). \quad (4)$$

In order to take into account edge effects, one sets

$$\begin{aligned} \omega(z) &= \begin{cases} \left[1 - \left(\frac{2z}{W_m} \right)^2 \right]^{-1/2} & |z| < \frac{W_m}{2} \\ 0 & \text{elsewhere} \end{cases} \\ \delta(x) &= \begin{cases} \left[1 - \left(\frac{2x}{W_s} \right)^2 \right]^{-1/2} & |x| < \frac{W_s}{2} \\ 0 & \text{elsewhere.} \end{cases} \end{aligned}$$

The longitudinal dependence of the current in the strip is expanded in piecewise sinusoidal (PWS) functions as

$$E(x) = \sum_{n=1}^N I_n E_n(x) \quad (5)$$

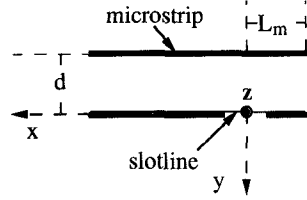


Fig. 2. Cross-sectional view of microstrip-to-slotline transition.

with

$$E_n(x) = \begin{cases} \frac{\sin k_e(H-|x-x_n|)}{\sin k_e H} : |x-x_n| < H, & |z| < \frac{W_m}{2} \\ 0 & \text{elsewhere.} \end{cases}$$

Here $x_n = -L_m + nH$ and H , are the center and the half-length of the PWS mode respectively; W_m and L_m are the length and the terminal location of the microstrip (Fig. 1). The choice of k_e is the same as in [2].

In analogous manner, for the magnetic current density on the slot we set:

$$M(z) = \sum_{n=1}^M V_n M_n(z) \quad (6)$$

with

$$M_n(z) = \begin{cases} \frac{\sin k_e(H-|z-z_n|)}{\sin k_e H} : |z-z_n| < H, & |x| < \frac{W_s}{2} \\ 0 & \text{elsewhere} \end{cases}$$

$$z_n = -L_s + nH.$$

A bottle-neck in the mathematical model is met when adopting an excitation term that represents as closely as possible the actual situation of fundamental mode incidence in the microstrip-slotline circuit, with disturbances in the near field.

With reference to [1], [2], there are four different expansions for the current density:

- 1) A term representing a propagating guided mode in microstrip, with propagation constant β_m , incident upon the discontinuity

$$I^{\text{inc}} = e^{j\beta_m x}. \quad (7)$$

- 2) A reflected guided mode propagating in microstrip away from the discontinuity

$$I^{\text{ref}} = -\Gamma e^{-j\beta_m x}. \quad (8)$$

- 3) A wave transmitted through the junction into the slotline fundamental mode of propagation constant β_s ;

$$V^T = T e^{-j\beta_s z}. \quad (9)$$

- 4) A certain number of terms as in (3)–(4) in order to model the disturbance of the current in the neighborhood of the junction.

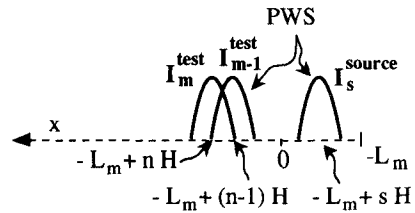


Fig. 3. Qualitative interpretation of the Galerkin method in solving (1.1) and (1.2).

As remarked before, the radiation (non-guided) field is only considered near the junction, assuming at a certain distance, the fundamental mode to be present.

The discretization of the integral (1)–(2) by the moments method leads to the following system of $M + N + 2$ linear equations:

$$\begin{bmatrix} [Z] & [Z^\Gamma] & [A^T] & [A^{12}] \\ [A^{21}] & [A^\Gamma] & [Y^T] & [Y] \end{bmatrix} \cdot \begin{bmatrix} [I] \\ -\Gamma \\ [V] \\ T \end{bmatrix} = \begin{bmatrix} [I^{\text{inc}}] \\ [V^{\text{inc}}] \end{bmatrix}. \quad (10)$$

The rather complicated elements of the matrix blocks and of the column vectors, obtainable from the integrals in [2], are not repeated here for the sake of brevity.

III. FUNDAMENTAL MODE BEHAVIOR

Upon consideration of the above integrals, one notices the large number of coefficients of different kinds that are involved in solving system (10).

In particular, the coefficients that present the greatest difficulty in implementation and require the largest computer times are those of the current sources relative to the fundamental mode; in [2] these are defined by the integrals (15), (17), (20)–(23).

In the present approach the evaluation of these integrals is circumvented by using an expansion in terms of piecewise sinusoidal functions, only (PWS), and avoiding the use of the exponentials (7)–(9).

Fig. 3 demonstrates the technique adopted. Taking as x the longitudinal axis of the microstrip (or slotline), the contribution to the electric field $E_x(x, -d, z)$, given by a single PWS-function, I_s^{source} , is seen through the test PWS-function, I_n^{test} . Due to the decay of the electric field produced by I_s^{source} , it is evident that the scalar product with I_n^{test} is of lesser magnitude than that with the $(n-1)$ th test function I_{n-1}^{test} , for the latter is closer to the source.

Fig. 4 gives the variation of the coupling coefficients Z_{ns} , between a test function and a source located along the same line, versus their mutual distance.

Analogous considerations and results hold when the PWS-source and test functions are located on different lines (Fig. 5).

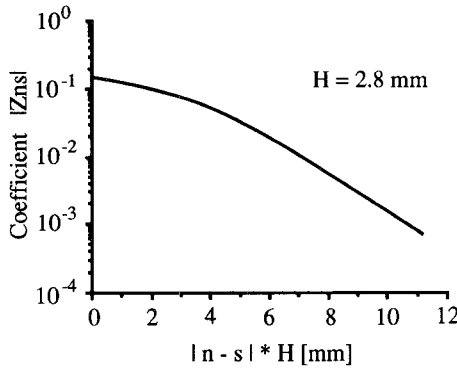


Fig. 4. Decay of the magnitude $|Z_{ns}|$ versus distance between I_s^{source} and I_n^{test} with $H = 0.028 \lambda_0$ and $f = 3$ GHz.

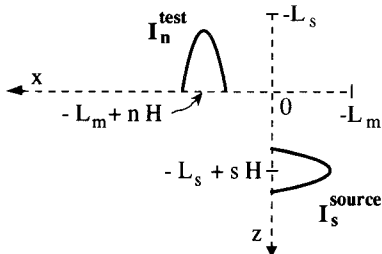


Fig. 5. Qualitative interpretation of the moments method when test and source functions refer to different lines.

In this second case, we can also plot the magnitude of A_{ns}^{12} , having fixed $s = 0$, while letting the n th test function vary (Fig. 6).

In the light of the above considerations, instead of using the expansions (7)–(9), we carry out a PWS sampling of the fundamental mode, that we consider to be present at a certain distance from the discontinuity.

We take, in fact, the following expression for the unknown current density over the microstrip

$$J_x(x, -d, z) = \sum_{s=1}^N I_s E_s(x) \omega(z) \quad (11)$$

and observing that

$$J_x(-L_m + sH, -d, z) = I_s \omega(z)$$

we remark that, after a sufficiently large value $s = k$, the s th coefficient of the longitudinal expansion (11) is given by

$$I_s = e^{j(-L_m + sH)\beta_m} - \Gamma e^{-j(-L_m + sH)\beta_m}. \quad (12)$$

Identical considerations hold for the magnetic current density, along the slotline, so that we have

$$E_x(x, 0, z) = \sum_{s=1}^M V_s M_s(z) \delta(x) \quad (13)$$

while

$$E_x(x, 0, -L_s + sH) = V_s \delta(x).$$

Hence, as from a given value $s = k$, we have

$$V_s = T e^{-j(-L_s + sH)\beta_s}. \quad (14)$$

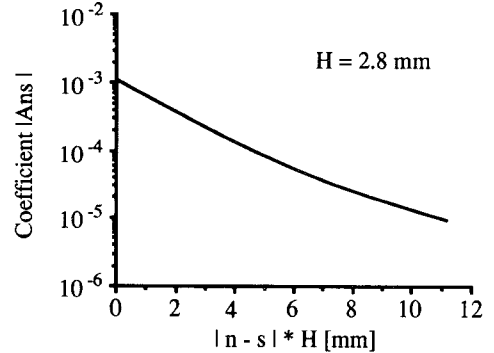


Fig. 6. Decay of magnitude A_{ns}^{12} versus distance between I_s^{source} and I_n^{test} with $H = 0.028 \lambda_0$ and $f = 3$ GHz.

Finally, we obtain the following sampled decompositions of the unknown electric and magnetic currents

$$\begin{aligned} J_x(x, -d, z) &= \sum_{s=1}^{k-1} I_s E_s(x) \omega(z) + \\ &+ \sum_{s=k}^{K_{\max}} [e^{j(-L_m + sH)\beta_m} - \Gamma e^{-j(-L_m + sH)\beta_m}] E_s(x) \omega(z) \end{aligned} \quad (15)$$

and

$$\begin{aligned} E_x(x, 0, z) &= \sum_{s=1}^{k-1} V_s M_s(z) \delta(x) + \\ &+ \sum_{s=k}^{K_{\max}} T e^{-j(-L_s + sH)\beta_s} M_s(z) \delta(x). \end{aligned} \quad (16)$$

Recalling the previous considerations about the decay of the contributions to the field $E_x(x, -d, z)$ and to the current $J_x(x, 0, z)$, the value of K_{\max} is determined as the minimum value that achieves convergence in the results.

In our numerical examples, in fact, a convergent solution is achieved computing the same number of coefficients in the integrals (14), (16), (18) in [2], with $N = M = 4$, $k = N + 1$ and $H = 0.03 * \lambda_0$.

It is important to remark, however, that by means of the above fundamental mode sampling, one avoids the computation of six different kinds of coefficients, namely, those defined by the integrals (15)–(17), (21)–(23) in [2], which also involve the greatest numerical effort.

The method described allows the solution to be reached by computing just three types of integrals, namely (14), (16), (18), out of the nine kinds occurring in [2], which, moreover, are the easiest to evaluate.

We are then reduced to the following column vectors:

1) $[Z^\Gamma]$ is a $(N + 1) \times 1$ column vector with elements,

$$Z_n^\Gamma = \sum_{s=k}^{K_{\max}} e^{-j(-L_m + sH)\beta_m} Z_{ns} \quad (17a)$$

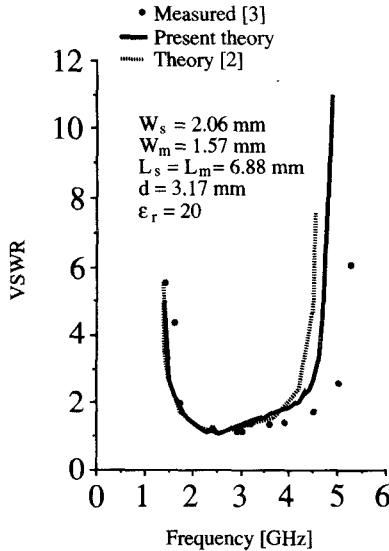


Fig. 7. VSWR versus frequency for microstrip-slotline transition.

2) $[A^T]$ is a $(N+1) \times 1$ column vector with elements,

$$A_n^T = \sum_{s=k}^{K_{\max}} [e^{-j(-L_s + sH)\beta_s} A_{ns}^{12}] \quad (17b)$$

3) $[A^\Gamma]$ is a $(M+1) \times 1$ column vector with elements,

$$A_n^\Gamma = \sum_{s=k}^{K_{\max}} e^{-j(-L_m + sH)\beta_m} A_{ns}^{21} \quad (17c)$$

4) $[Y^T]$ is a $(M+1) \times 1$ column vector with elements,

$$Y_n^T = \sum_{s=k}^{K_{\max}} [e^{-j(-L_s + sH)\beta_s} Y_{ns}]. \quad (17d)$$

The driving term in the system (1.8) is given by the following column vector:

1) $[I^{\text{inc}}]$ is a $(N+1) \times 1$ column vector with elements,

$$I_n^{\text{inc}} = - \sum_{s=k}^{K_{\max}} e^{j(-L_m + sH)\beta_m} Z_{ns} \quad (18a)$$

2) $[V^{\text{inc}}]$ is a $(M+1) \times 1$ column vector with elements,

$$V_n^{\text{inc}} = - \sum_{s=k}^{K_{\max}} e^{j(-L_m + sH)\beta_m} A_{ns}^{21}. \quad (18b)$$

In the above expansions, Z_{ns} corresponds to the integral (14), Y_{ns} to (16) and A_{ns}^{12} to (18) of [2] (A_{ns}^{12} is given by (19)). The elements of the block matrices $[Z]$, $[A^{12}]$, $[A^{21}]$, $[Y]$, are the same as in [2].

IV. RESULTS

A. Microstrip-to Slotline Transition

Fig. 7 shows the behavior of the VSWR for the junction of Fig. 1 where

$$\text{VSWR} = \frac{1 + |\Gamma|}{1 - |\Gamma|}.$$

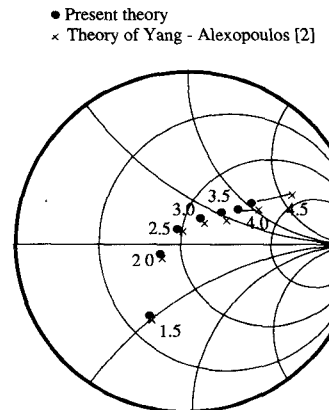


Fig. 8. Smith chart plot of impedance versus frequency [GHz] for microstrip-slotline transition. The reference plane is at the center of the cross section.

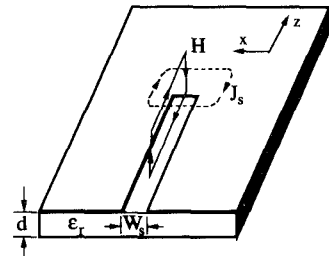


Fig. 9. Short-circuited slotline, with the magnetic field and surface current distribution [4].

By comparing the results of the present method with the theoretical results of [2] and with the measurements reported in [4], we notice a broadening of the band pass predicted by our model, in slightly closer agreement with [4].

Further checks were carried out with regard to the driving point impedance of the junction, by comparing our results with the numerical data of [2].

In Fig. 8 we can see very good agreement with the above theory, except that a somewhat higher band edge is predicted by our results.

B. Shorted-End Slotline

The mathematical model previously developed is well suited to the study of different kinds of discontinuities. Fig. 9 depicts the configuration of "short-circuited" slotline, showing the magnetic field lines and the surface electric current distribution, as from [3]. The current flows around the termination and it is reasonable to assume that storage of magnetic energy takes place in this region. Consequently, an inductive reactance is located at the slot end, as shown in the equivalent circuit of Fig. 10.

Beside the reactance, a resistance load is also included in order to take into account losses due to radiation and surface waves.

Upon consideration of Fig. 9, we notice that, unlike in the case of the previous junction, the discontinuity takes

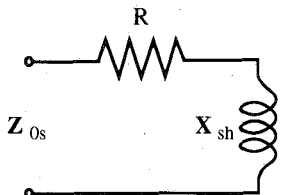


Fig. 10. Equivalent circuit of short-end termination in slotline.

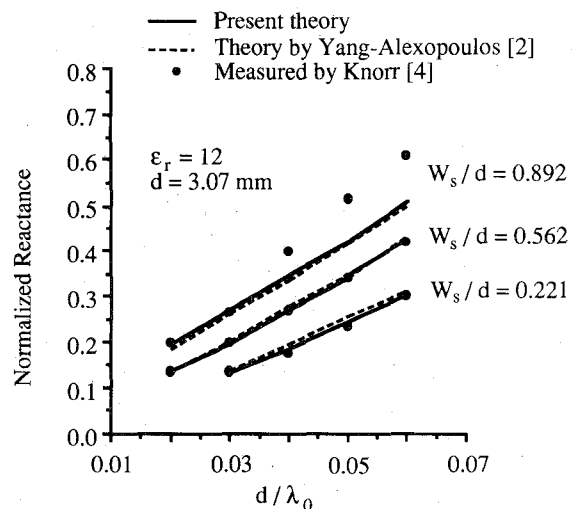
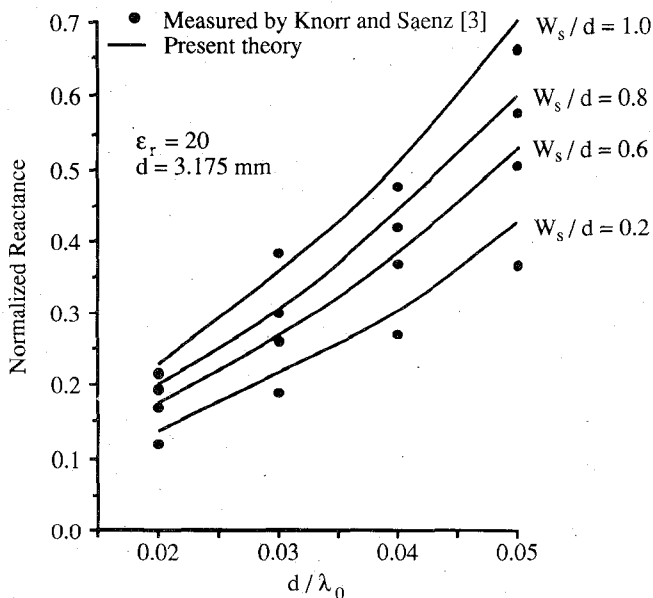


Fig. 11. Normalized reactance of short-end slotline, versus ratio substrate thickness/wavelength in vacuo.

Fig. 12. Normalized reactance of short-end slotline, with $\epsilon_r = 20$.

place at a single interface. A single integral equation, therefore, is involved in this case.

Our technique reduces considerably the numerical effort involved in studying this discontinuity: on a MICROVAX 3600 system, we obtain the reflection coefficient Γ , for a given frequency, in about 25" of CPU-time.

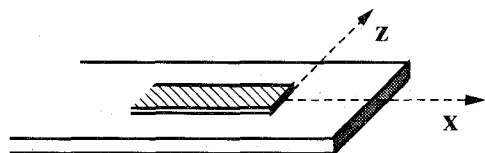


Fig. 13. Geometry of an open-end microstrip.

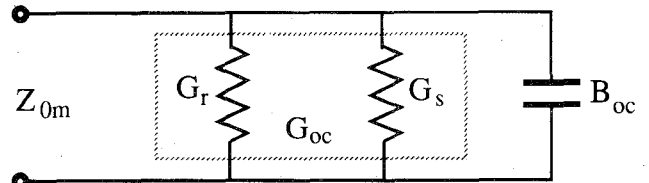


Fig. 14. Equivalent circuit of an open-end termination in microstrip.

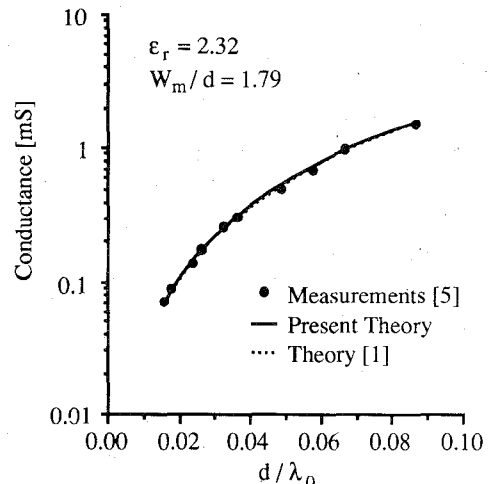


Fig. 15. Conductance of open-end microstrip.

By utilizing the standard formula:

$$\bar{Z}_{sh} = \frac{Z_{sh}}{Z_{0s}} = \frac{1 + \Gamma}{1 - \Gamma}$$

we recover the equivalent impedance of a short-circuited slot, normalized to the characteristic impedance of the line. We report in Fig. 11 the variation of the normalized reactance versus the ratio substrate thickness/wavelength in vacuo. The agreement between the results of Yang-Alexopoulos theory and ours, obtained by fundamental mode sampling, is very good. The agreement with the experimental data of [2] is also good for slot widths W_s somewhat larger than the substrate thickness.

More experimental data being available with

$$\epsilon_r = 20; d = 3.175 \text{ mm} [3]$$

we also carried out a simulation with these parameters and for different values of the W_s/d ratio (see Fig. 12), always with excellent agreement.

C. Open-End Microstrip

A problem of great interest is posed by the accurate characterization of the frequency behavior of an open end microstrip, whose geometry is reported in Fig. 13.

The equivalent circuit of an open-end termination in microstrip is shown in Fig. 14.

The adaptation of the theoretical model to this problem proceeds in a manner very similar to that followed for the "dual" case of short circuit termination in slotline. Here again, we compute the reflection coefficient Γ .

The admittance of the termination is obtained from

$$Y_{oc} = (G_r + G_s) + jB_{oc} = \frac{1 - \Gamma}{1 + \Gamma} \frac{1}{Z_{0m}}$$

where G_r and G_s distinguish the radiation and surface wave conductances.

Fig. 15 compares the conductance of open end microstrip, as obtained with our method, with the numerical data of [1] and the experimental data of [5]. A number of similar comparisons were carried out yielding similar results.

V. CONCLUSION

We present a modified version of the moments method for planar circuits simulation, based on "fundamental mode sampling." The results obtained by this technique feature good agreement with experiment and particularly much reduced numerical effort and computation times.

We believe this approach will enhance the applicability of an already very useful and flexible method.

REFERENCES

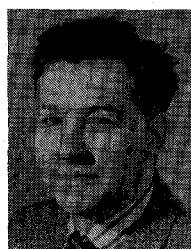
- [1] R. W. Jackson and D. M. Pozar, "Full wave analysis of microstrip open-end and gap discontinuities," *IEEE Trans. Microwave Theory Tech.*, vol. MTT-33, pp. 1036-1042, Oct. 1985.
- [2] Hung-Yu Yang and N. G. Alexopoulos, "A dynamic model for microstrip-slotline transition and related structures," *IEEE Trans. Microwave Theory Tech.*, pp. 286-292, vol. MTT-36, Feb. 1988.
- [3] K. G. Gupta, R. Garg, and I. J. Bahl, "Microstrip lines and slotlines," Norwood, MA: Artech House, 1979.
- [4] J. B. Knorr, "Slot-lines transitions," *IEEE Trans. Microwave Theory Tech.*, vol. MTT-22, pp. 548-554, May 1974.
- [5] J. R. James, P. S. Hall and C. Wood, *Microstrip Antenna Theory and Design*. London: Peregrinus, 1981.



Tullio Rozzi (M'66-SM'74-F'90) was born in Italy in 1941. He obtained the degree of dottore in Physics from Pisa University in 1965, the Ph.D. degree in electrical engineering from Leeds University in 1968 and the D.Sc. degree from the University of Bath in 1987.

From 1968 to 1978 he was a Research Scientist at the Philips Research Laboratories, Eindhoven, The Netherlands, having spent one year, 1975, at the Antenna Laboratory, University of Illinois, Urbana. In 1978 he was appointed to Chair of Electrical Engineering at University of Liverpool, U.K., and subsequently was appointed to the Chair of Electronics and Head of the Electronics Group at the University of Bath in 1981. From 1983 to 1986 he held the additional responsibility of Head of School of Electrical Engineering at Bath. Since 1988 he has held the Chair of Antennas at the Faculty of Engineering, University of Ancona, Ancona, Italy, while remaining a visiting professor at Bath.

In 1975 Dr. Rozzi was awarded the Microwave Prize by the Microwave Theory and Techniques Society of the IEEE. He is also Fellow of the IEE (U.K.).



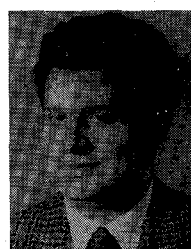
Antonio Morini was born in Italy in 1962. He received the degree of Dottore Ingegnere in Electronics Engineering from the University of Ancona in 1987.

Since 1988 he has been with the Dipartimento di Elettronica ed Automatica at the University of Ancona as a researcher assistant. His research is mainly devoted to the modeling of passive millimetric wave devices and antennas.



Andrea Pallotta was born in Ancona, Italy, in 1962. He received the degree of Dottore Ingegnere in electronics engineering from the University of Ancona in 1990 and is currently working at Italtel, Milan.

His research is mainly devoted to the design of microwave circuits.



Franco Moglie (M'91) was born in Ancona, Italy, in 1961. He received the degree of Dottore Ingegnere in Electronics Engineering from the University of Ancona, Italy, in 1986.

Since 1986 he has been a tenured Researcher with the Dipartimento di Elettronica ed Automatica at the same University. His work is mainly in the area of Microwave and Millimetre Techniques and Hyperthermia Applicators.